# Journal of Materials Chemistry A

Accepted Manuscript


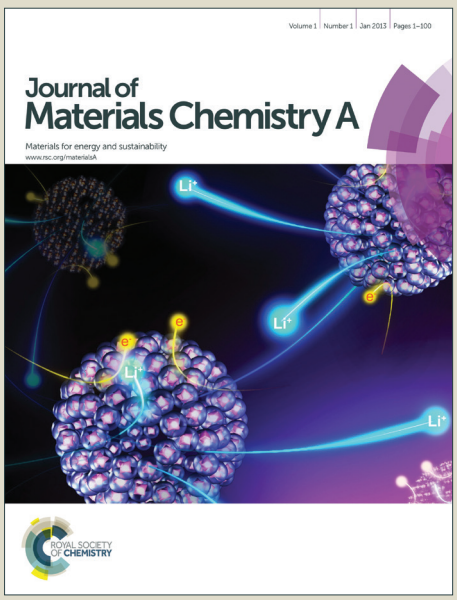





ROYAL SOCIETY OF CHEMISTRY

www.rsc.org/materialsA

Journal of Materials Chemistry A

RSCPublishing

ARTICLE

# Efficient Quasi-Solid-State Dye-Sensitized Solar Cells Based on Organic Sensitizers Containing Fluorinated Quinoxaline Moiety

Xiaowei Jia,† Weiyi Zhang,† Xuefeng Lu, Zhong-Sheng Wang, and Gang Zhou*

Cite this: DOI: 10.1039/x0xx00000x

Received 00th January 2012,
Accepted 00th January 2012

DOI: 10.1039/x0xx00000x

www.rsc.org/

Two novel organic sensitizers (**FNE55** and **FNE56**) containing 6,7-difluoroquinoxaline moiety have been designed and synthesized for quasi-solid-state dye-sensitized solar cells (DSSCs). For comparison, organic dye **FNE54** without fluorine has also been synthesized. The effects of the introduction of fluorine on the absorption, electrochemical and photovoltaic properties have been systematically investigated. Upon the incorporation of fluorine on the quinoxaline unit, the electron-withdrawing ability is strengthened, which results in the enhanced push-pull interactions and thus narrowed energy band gap. The absorption maximum wavelength in toluene solution bathochromically shifts from 504 nm for **FNE54** to 511 nm for **FNE55**, and further to 525 nm for **FNE56**. However, although the lowest unoccupied molecular orbitals (LUMOs) are lowered down after the introduction of fluorines, the driving force for the photo-excited electrons from their excited states to the semiconductor conduction band is still enough. Consequently, the quasi-solid-state DSSC based on **FNE56** exhibits a highest power conversion efficiency of 8.2%, which is 37% higher than that for **FNE54** based quasi-solid-state DSSC.

## Introduction

Dye-sensitized solar cells (DSSCs),[1] regarded as one of the most promising photovoltaic devices, have been extensively investigated due to their high theoretical efficiency, facile fabrication processes, and potential low cost. Over the past two decades, continuous research efforts have contributed to the great advances in the DSSC performance.[2] Up to date, DSSC devices employing zinc-porphyrin co-sensitized system have shown an efficiency record of 13% under standard global air mass 1.5.[3] However, most highly efficient DSSCs have been realized with volatile organic liquid electrolytes, which may limit their outdoor applications. In view of promising commercial application, alternatively, quasi-solid-state DSSCs[4] with non-flowing and non-volatile electrolyte have shown greatly improved long-term stability as there is less or no possibility of electrolyte leakage.

To achieve high DSSC performance, in addition to the innovation and optimization in the device structure and processing, one of the most critical contributions is the material development. Therefore, substantial efforts have focused on the optimization of metal-free organic sensitizer with reduced energy gap and enhanced molar absorption coefficient. Decreasing the band gap can be achieved by either lowering the lowest unoccupied molecular orbital (LUMO) or raising the highest occupied molecular orbital (HOMO) of the organic sensitizer, or both. However, smaller band gap benefits the light-harvesting, but may result in insufficient electron injection from the excited state to the titania conduction band due to the unsuitable LUMO levels of the organic sensitizers. Therefore, it is generally considered that a minimum offset of around 0.3 eV between the LUMO of the organic sensitizer and the conduction band edge of titania semiconductor, which determines the driving force for the excited electron injection, is needed to ensure fast and efficient electron injection.[5] As a consequence, tuning the LUMO energy levels of the organic sensitizers with respect to the acceptor is of great importance to optimize the DSSC performance.

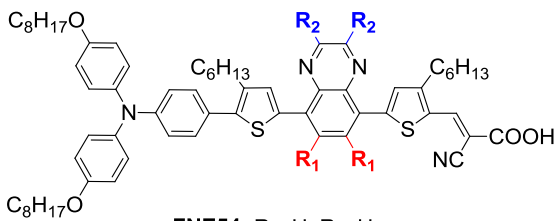


**FNE54:** $R_1$=H; $R_2$=H

**FNE55:** $R_1$=F; $R_2$=H

**FNE56:** $R_1$=F; $R_2$=Ph

**Fig. 1** Chemical structures of sensitizers **FNE54**, **FNE55**, and **FNE56**.

Fluorine is the most electronegative element and the smallest electron-withdrawing group, with great influence on inter- and intramolecular interactions through C–F···H, F···S, and C–F···$\pi_F$ interactions.[6] Consequently, introduction of fluorine atoms (van der Waals radius, $r$ = 1.35 Å, only slightly larger

than hydrogen, $r$ = 1.2 Å) into the conjugation system has small effect on the molecular geometry structure. However, the substitution of fluorine for hydrogen can significantly affect the optoelectronic properties of the π-conjugated molecules due to the lower LUMO levels as compared with the non-fluorinated analogs. As a result, fluorinated conjugated materials have been widely utilized in various applications, such as light-emitting diode (LED),[7] field-effect transistor (FET)[8] and bulk heterojunction polymer solar cell (PSC).[9] However, there are only a few examples of applying fluorinated compounds in DSSC.[10]

Recently, D-A'-π-A featured organic sensitizers,[11] where an auxiliary acceptor (A'), such as benzothiadiazole,[3,12] diketopyrrolopyrrole,[13] pyridopyrazine,[14] and quinoxaline,[15] is integrated into the traditional D-π-A framework, have been extensively investigated. Bathochromically shifted absorption band of the organic sensitizer can be achieved due to the enhanced donor-acceptor interactions, which results in an increased light harvesting efficiency. Most importantly, tunable HOMO levels along with enhanced photostability of the organic sensitizers can be achieved upon the incorporation of the auxiliary acceptor. Among the various implemented electron-withdrawing groups,[3,12-15] quinoxaline unit has been embedded into the organic sensitizers as an auxiliary electron acceptor for efficient DSSCs by several groups including our own.[15] All the previous results indicates that the LUMO levels of the quinoxaline based organic sensitizers can be further lowered down to harvest more solar photons while the photo-generated electrons can be still effectively injected into the titania conduction band with the presence of enough electron injection driving force. Herein, we report two fluorinated organic sensitizers (**FNE55** and **FNE56**, Fig. 1) containing 6,7-difluoroquinoxaline moiety as electron acceptor and their applications in quasi-solid-state DSSCs. For comparison, sensitizer **FNE54** without fluorine has also been synthesized. The effects of the introduction of fluorine on the absorption, electrochemical and photovoltaic properties have been systematically investigated. It is found that the incorporation of two fluorines on quinoxaline unit have successfully lowered down the LUMO level of the organic sensitizers, which results in the narrowed band gap. On the other hand, the driving force for the photo-excited electrons from their excited states to the semiconductor conduction band is still enough. Therefore, **FNE56** based quasi-solid-state DSSC displays a highest $\eta$ of 8.2%, which is 37% higher than that for the quasi-solid-state DSSC based on sensitizer **FNE54**.

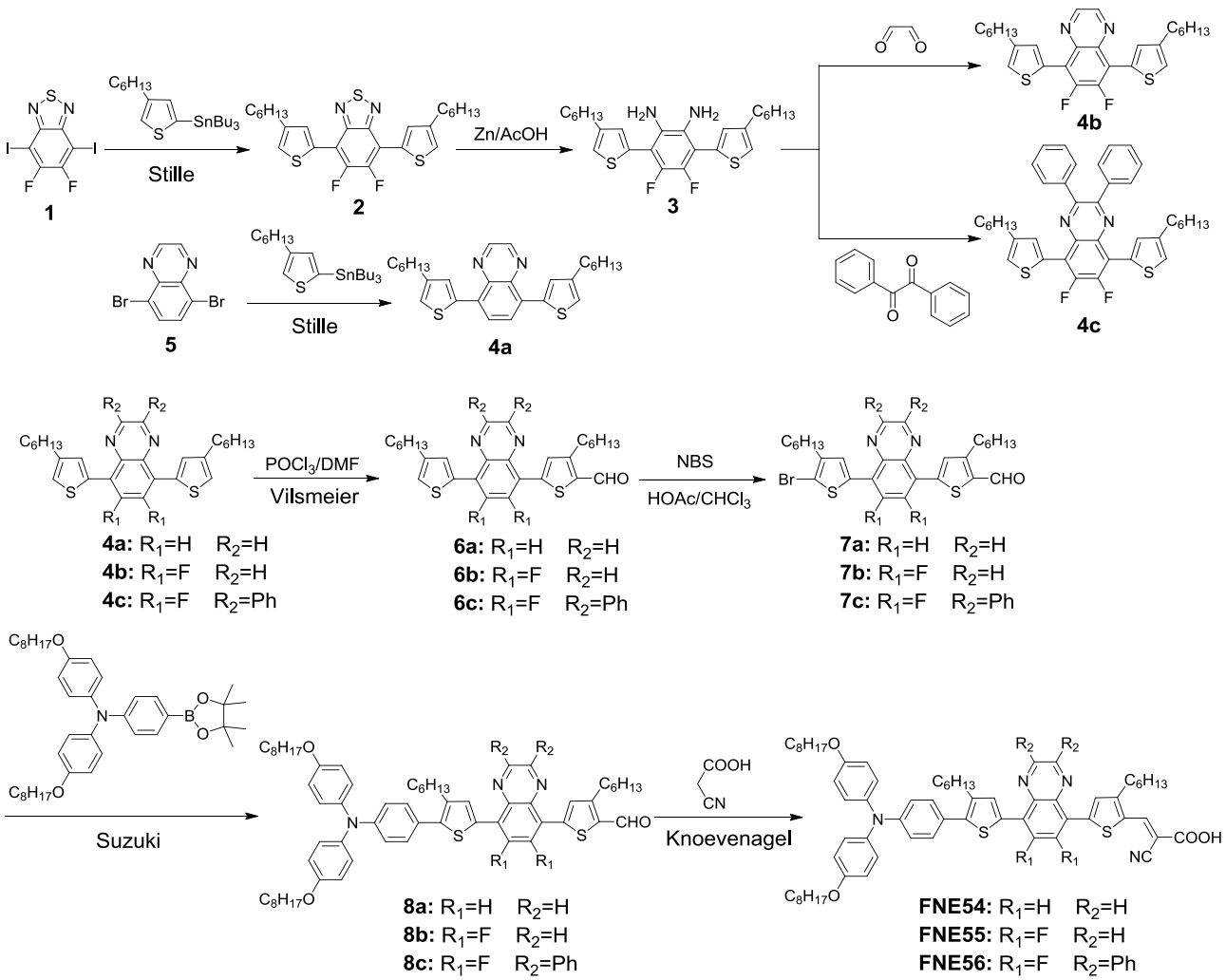


**Scheme 1** Synthetic routes for sensitizers **FNE54**, **FNE55**, and **FNE56**.



 

## Experimental Section

**Materials and Reagents.** 4,5-Difluoro-2-nitroaniline, glyoxal (40 wt% solution in $H_2O$), benzil, thiophene and *N*-bromosuccinimide (NBS) were purchased from J&K Chemical Ltd, China. Purification of organic solvents used in this work was under the standard process. Other chemicals and reagents were used as received from commercial suppliers without further purification. Transparent conductive glass (F-doped $SnO_2$, FTO, 15 Ω per square, transmittance of 80%, Nippon Sheet Glass Co., Japan) was used as the substrate for the fabrication of DSSC.

**Synthesis of compound 2.** Under nitrogen atmosphere, a mixture of compound **1**[16] (1.4 g, 3.3 mmol), tributyl(4-hexylthien-2-yl)stannane (4.57 g, 10.0 mmol), $Pd(PPh_3)_4$ (150 mg, 0.13 mmol) and toluene (150 mL) was stirred and heated at 88 ℃ for 12 h. After removal of excess solvent, the residue was purified by flash column chromatography (silica gel, DCM / PE = 1/5). Yellow solid **2** was obtained with a yield of 72% (1.2 g). $^1$H NMR (400 MHz, $CDCl_3$, $\delta$ ppm): 8.11 (s, 2H), 7.20 (s, 2H), 2.71 (t, 4H, $J$ = 8 Hz), 1.70 (m, 4H), 1.34 (m, 12H), 0.90 (t, 6H, $J$ = 8 Hz). $^{19}$F NMR (376 MHz, $CDCl_3$, $\delta$ ppm): -128.65 (s, 2F). $^{13}$C NMR (100 MHz, $CDCl_3$, $\delta$ ppm): 223.5, 151.4, 148.8, 147.6, 143.9, 132.5, 131.4, 124.2, 31.9, 30.7, 29.3, 22.9, 14.4.

**Synthesis of compound 4a.** Under nitrogen atmosphere, a mixture of compound **5**[17] (566 mg, 1.96 mmol), tributyl(4-hexylthien-2-yl)stannane (2.24 g, 4.9 mmol) and $Pd(PPh_3)_4$ (80 mg, 0.07 mmol) in *N*,*N*-dimethylformamide (DMF) (20 mL) was stirred and heated at 85 ℃ for 12 h. After removal of the solvent, the residue was purified by flash column chromatography (silica gel, DCM/PE = 1/3). Yellow solid **4a** was obtained with a yield of 55% (500 mg). $^1$H NMR (400 MHz, $CDCl_3$, $\delta$ ppm): 8.96 (s, 2H), 8.09 (s, 2H), 7.66 (s, 2H), 7.10 (s, 2H), 2.69 (t, 2H, $J$ = 7.7 Hz), 1.73-1.66 (m, 4H), 1.42-1.32 (m, 12H), 0.90 (t, 6H, $J$ = 6.9 Hz). $^{13}$C NMR (100 MHz, $CDCl_3$, $\delta$ ppm): 143.7, 143.4, 140.2, 138.4, 132.4, 129, 128, 123.6, 32, 30.8, 30.8, 29.3, 22.9, 14.4.

**Synthesis of compound 4b.** A suspension of zinc dust (1.57 g, 24 mmol) and compound **2** (493 mg, 0.98 mmol) in acetic acid (60 mL) was stirred at 60 ℃ for 24 h and the excess zinc was removed by filtration. The filtrate was transferred to a separatory funnel, extracted with DCM and then washed with diluted sodium hydroxide solution and brine until water phase was neutralized. After removal of the solvent, pale yellow liquid **3** was obtained. As amine **3** is unstable, after a few drops of triethylamine was added, **3** was instantly condensed with glyoxal (229 mg, 3.95 mmol) in ethanol solution for 12 h. Removal of the solvent gave a crude product which was purified by flash column chromatography (silica gel, DCM/PE = 1/3). Yellow solid **4b** was obtained with a yield of 45 % (220 mg). $^1$H NMR (400 MHz, $CDCl_3$, $\delta$ ppm): 8.94 (s, 2H), 7.74 (s, 2H), 7.23 (s, 2H), 2.71 (t, 4H, $J$ = 7.6 Hz), 1.73-1.66 (m, 4H), 1.28-1.25 (m, 12H), 0.91-0.86 (m, 6H). $^{19}$F NMR (376 MHz, $CDCl_3$, $\delta$ ppm): -128.47. $^{13}$C NMR (100 MHz, $CDCl_3$, $\delta$ ppm): 143.3, 141.6, 133.6, 132.8, 132.7, 130.1, 128.6, 125.1, 31.9, 30.7, 29.3, 27.4, 22.9, 14.3.

**Synthesis of compound 4c.** Compound **4c** was synthesized similarly as described for compound **4b**. Red solid, yield 92 % (500 mg). $^1$H NMR (400 MHz, $CDCl_3$, $\delta$ ppm): 7.88 (s, 2H), 7.75-7.69 (m, 4H), 7.43-7.32 (m, 6H), 7.23 (s, 2H), 2.71 (t, 4H, $J$ = 7.7 Hz), 1.76-1.63 (m, 4H), 1.45-1.27 (m, 12H), 0.90 (t, 6H, $J$ = 6.9 Hz). $^{19}$F NMR (376 MHz, $CDCl_3$, $\delta$ ppm): -129.46. $^{13}$C NMR (100 MHz, $CDCl_3$, $\delta$ ppm): 151.5, 148.6, 143.0, 138.4, 135.1, 132.7, 132.6, 132.5, 130.7, 129.4, 128.5, 125.4, 32.0, 30.8, 30.7, 29.3, 22.9, 14.4.

**Synthesis of 6a.** After cooling a solution of compound **4a** (354 mg, 0.76 mmol) in DMF (40 mL) to 0 $^o$C, phosphorus oxychloride (1 mL, 10.9 mmol) was added dropwise. The reaction was kept at 80 $^o$C for 14 h under $N_2$. After cooling to room temperature, 30 mL saturated sodium acetate aqueous solution was added into the reaction mixture. The mixture was extracted with DCM, and the organic phase was collected and dried over anhydrous sodium sulfate. The solvent was removed with a rotary evaporator and the residue was purified on a silica gel column with DCM/PE (1/1, v/v) as eluent. Yellow solid **6a** was obtained with a yield 80 % (300 mg). $^1$H NMR (400 MHz, $CDCl_3$, $\delta$ ppm): 10.11 (s, 1H), 8.99 (d, 2H, $J$ = 7.5Hz), 8.19 (d, 1H, $J$ = 8.0 Hz), 8.12 (d, 1H, $J$ = 8.2 Hz), 7.71 (d, 2H, $J$ = 5.4 Hz), 7.15 (s, 1H), 3.02 (t, 2H, $J$ = 7.6 Hz), 2.69 (t, 2H, $J$ = 7.5 Hz), 1.82-1.63 (m, 4H), 1.49-1.22 (m, 12H), 0.90 (s, 6H). $^{13}$C NMR (100 MHz, $CDCl_3$, $\delta$ ppm): 183.0, 152.5, 147.1, 144.1, 144.0, 143.6, 140.2, 140.0, 139.3, 137.9, 134.3, 130.4, 130.1, 129.6, 128.7, 127.5, 124.6, 32.0, 31.9, 31.8, 31.8, 30.8, 29.3, 28.8, 22.9, 22.8, 14.4, 14.3.

**Synthesis of compound 6b.** Compound **6b** was synthesized similarly as described for compound **6a**. Yellow solid, yield 60% (133 mg). $^1$H NMR (400 MHz, $CDCl_3$, $\delta$ ppm): 10.16 (s, 1H), 8.99 (d, 2H, $J$ = 1.6 Hz), 7.81 (s, 2H), 7.28 (s, 1H), 3.04 (t, 2H, $J$ = 7.2 Hz), 2.72 (t, 2H, $J$ = 7.6 Hz), 1.77-1.68 (m, 4H), 1.34-1.26 (m, 12H), 0.9 (t, 6H, $J$ = 6.8 Hz). $^{19}$F NMR (376 MHz, $CDCl_3$, $\delta$ ppm): -126.10 (d, $J$ = 18.1 Hz), -128.34 (d, $J$ = 18.1 Hz). $^{13}$C NMR (100 MHz, $CDCl_3$, $\delta$ ppm): 182.9, 152.4, 152.0, 151.9, 151.7, 150.6, 150.4, 149.3, 149.2, 147.8, 141.8, 139.8, 139.1, 137.7, 134.9, 128.6, 128.6, 68.5, 32.1, 31.9, 31.8, 31.3, 29.9, 29.6, 29.5, 29.3, 26.3, 22.9, 14.4.

**Synthesis of compound 6c.** Compound **6c** was synthesized similarly as described for compound **6a**. Deep red solid, yield 55 % (287 mg). $^1$H NMR (400 MHz, THF-$d_8$, $\delta$ ppm): 10.14 (s, 1H), 7.91 (s, 1H), 7.88 (s, 1H), 7.73-7.69 (m, 4H), 7.46-7.34 (m, 6H), 7.28 (s, 1H), 3.02 (t, 2H, $J$ = 7.6 Hz), 2.70 (t, 2H, $J$ = 7.6 Hz), 1.79-1.66 (m, 4H), 1.46-1.30 (m, 12H), 0.92-0.89 (m, 6H). $^{19}$F NMR (376 MHz, THF-$d_8$, $\delta$ ppm): -125.25 (d, $J$ = 17.1 Hz), -127.44 (d, $J$ = 17.1 Hz). $^{13}$C NMR (100 MHz, $CDCl_3$, $\delta$ ppm): 183.0, 152.1, 152.0, 151.8, 150.7, 150.5, 149.5, 149.3, 148.1, 147.9, 143.1, 139.8, 139.4, 138.1, 137.9, 134.1, 133.9, 133.3, 133.2, 130.7, 130.6, 130.3, 129.7, 129.6, 128.7, 128.5, 126.4, 125.3, 120.1, 32.0, 31.9, 31.7, 30.8, 30.7, 29.3, 29.2, 28.7, 22.9, 22.8, 14.4, 14.2.

**Synthesis of compound 7a.** Under nitrogen atmosphere, compound **6a** (245 mg, 0.50 mmol) was dissolved in a mixed solution (40 mL) of $CHCl_3$/$CH_3COOH$(5/1, v/v). To this solution, NBS (100 mg, 0.56 mmol) was added. After the mixture was stirred at room temperature overnight, distilled water was added to quench the reaction. The solution was extracted with DCM for three times. The combined organic solution was washed with sodium hydroide solution and brine and dried over anhydrous sodium sulfate. The solvent was removed with a rotary evaporator and the residue was purified on a silica gel column with DCM/PE (1/1, v/v) as eluent. Yellow solid **7a** was obtained with a yield of 86% (245 mg). $^1$H NMR (400 MHz, $CDCl_3$, $\delta$ ppm): 10.11 (s, 1H), 9.00 (d, 2H, $J$ = 3.2 Hz), 8.19 (d, 1H, $J$ = 8.1 Hz), 8.13 (d, 1H, $J$ = 8.0 Hz), 7.71 (s, 1H), 7.54 (s, 1H), 3.03 (t, 2H, $J$ = 7.7 Hz), 2.64 (t, 2H, $J$ = 7.7 Hz), 1.76-1.65 (m, 4H), 1.33-1.28 (m, 12H), 0.9 (t, 6H, $J$ = 6.8 Hz). $^{13}$C NMR (100 MHz, $CDCl_3$, $\delta$ ppm): 182.8, 152.4,

146.8, 146.5, 144.2, 143.6, 141.8, 139.4, 139.3, 130.2, 128.7, 127.6, 126.1, 31.9, 31.7, 30.0, 29.8, 29.3, 29.2, 28.8, 22.8, 14.3.

**Synthesis of compound 7b.** Compound **7b** was synthesized similarly as described for compound **7a**. Yellow solid, yield 86% (131 mg). $^1$H NMR (400 MHz, $CDCl_3$, $\delta$ ppm): 10.15 (s, 1H), 8.97 (d, 1H, $J$ = 1.6 Hz), 8.95 (d, 1H, $J$ = 1.6 Hz), 7.80 (s, 1H), 7.78 (s, 1H), 3.05 (t, 2H, $J$ = 7.6 Hz), 2.71 (t, 2H, $J$ = 7.6 Hz), 1.78-1.66 (m, 4H), 1.44-1.32 (m, 12H), 0.9 (t, 6H, $J$ = 6.8 Hz). $^{19}$F NMR (376 MHz, $CDCl_3$, $\delta$ ppm): -126.10 (d, $J$ = 18.1 Hz), -128.34 (d, $J$ = 18.1 Hz). $^{13}$C NMR (100 MHz, $CDCl_3$, $\delta$ ppm): 182.9, 154.4, 152.0, 151.9, 151.7, 150.6, 150.4, 149.3, 149.2, 148, 147.8, 141.8, 139.8, 139.1, 137.7, 134.9, 128.6, 128.6, 68.5, 32.1, 31.9, 31.9, 31.3, 29.9, 29.6, 29.5, 28.8, 26.3, 22.9, 14.4.

**Synthesis of compound 7c.** Compound **7c** was synthesized similarly as described for compound **7a**. Red solid, yield 70% (223 mg). $^1$H NMR (400 MHz, $CDCl_3$, $\delta$ ppm): 10.15 (s, 1H), 7.94 (s, 1H), 7.89 (s, 1H), 7.73-7.69 (m, 4H), 7.46-7.34 (m, 6H), 3.02 (t, 2H, $J$ = 7.6 Hz), 2.70 (t, 2H, $J$ = 7.6 Hz), 1.79-1.66 (m, 4H), 1.46-1.30 (m, 12H), 0.92-0.89 (m, 6H). $^{19}$F NMR (376 MHz, $CDCl_3$, $\delta$ ppm): -126.85 (d, $J$ = 16.7 Hz), -129.00 (d, $J$ = 16.6 Hz). $^{13}$C NMR (100 MHz, $CDCl_3$, $\delta$ ppm): 182.9, 152.4, 152.0, 151.9, 151.7, 150.6, 150.4, 149.3, 149.2, 148, 147.8, 141.8, 139.8, 139.1, 137.7, 134.9, 134.8, 134.4, 134.3, 134.1, 133.9, 132.5, 132.4, 130.7, 129.8, 129.7, 128.6, 128.5, 31.9, 31.6, 29.9, 29.8, 29.3, 29.2, 28.7, 22.9, 22.8, 14.4, 14.3.

**Synthesis of compound 8a.** Under nitrogen atmosphere, a mixture of compound **7a** (157 mg, 0.28 mmol), *N*,*N*-bis[4-(hexyloxy)phenyl]-4-(4,4,5,5-tetramethyl-1,3,2-dioxaborolan-2-yl)-aniline (73 mg, 0.25 mmol), $Pd(PPh_3)_4$ (27 mg, 0.02 mmol) and $K_2CO_3$ (2.76 g, 0.02 mol) in a mixed solution of water (5 mL), toluene (15 mL) and THF (15 mL) was stirred and heated at 85 ℃ for 24 h. When the reaction was completed, the mixture was extracted with DCM for three times. The combined organic solution was washed with brine and dried by anhydrous sodium sulfate. The solvent was removed with a rotary evaporator and the residue was purified on a silica gel column with DCM/PE (1/1, v/v) as eluent. Red solid **8a** was obtained with a yield 80% (149 mg). $^1$H NMR (400 MHz, $CDCl_3$, $\delta$ ppm): 10.11 (s, 1H), 8.98 (d, 2H, $J$ = 3.3 Hz), 8.18 (d, 1H, $J$ = 3.3 Hz), 8.13 (d, 1H, $J$ = 8.1 Hz), 7.75 (s, 1H), 7.70 (s, 1H), 7.32 (d, 2H, $J$ = 8.7 Hz), 7.10 (d, 4H, $J$ = 8.9 Hz), 6.96 (d, 2H, $J$ = 8.7 Hz), 6.85 (d, 4H, $J$ = 8.9 Hz), 3.94 (t, 4H, $J$ = 6.5 Hz), 3.02 (t, 2H, $J$ = 7.7 Hz), 2.78-2.68 (m, 2H), 1.84-1.62 (m, 8H), 1.52-1.20 (m, 32H), 0.96-0.85 (m, 12H). $^{13}$C NMR (100 MHz, $CDCl_3$, $\delta$ ppm): 182.9, 155.9, 152.4, 148.5, 147.2, 143.9, 143.8, 143.1, 140.6, 140.3, 139.9, 139.2, 138.3, 135.1, 134.2, 130.8, 129.9, 129.8, 129.4, 128.7, 127.1, 126.7, 126.3, 123.9, 119.9, 115.5, 68.5, 32.1, 31.9, 31.8, 31.3, 29.9, 29.6, 29.5, 29.3, 29.1, 28.8, 26.3, 22.9, 22.8, 14.4.

**Synthesis of compound 8b.** Compound **8b** was synthesized similarly as described for compound **8a**. Red solid, yield 86% (131 mg). $^1$H NMR (400 MHz, $CDCl_3$, $\delta$ ppm): 10.08 (s, 1H), 8.90 (s, 2H), 7.80 (s, 1H), 7.73 (s, 1H), 7.33 (d, 2H, $J$ = 8.2 Hz) 7.05 (d, 4H, $J$ = 8.6 Hz), 6.90 (d, 2H, $J$ = 8.2 Hz), 6.79 (d, 4H, $J$ = 8.5 Hz), 3.89 (t, $J$ = 6.5 Hz, 4H), 2.99 (t, $J$ = 7.8 Hz, 2H), 2.69 (t, $J$ = 7.9 Hz, 2H), 1.70 (m, 8H), 1.45-1.11 (m, 32H), 0.82 (t, $J$ = 5.6 Hz, 12H). $^{19}$F NMR (376 MHz, $CDCl_3$, $\delta$ ppm): -126.26 (d, $J$ = 16.7 Hz), -128.82 (d, $J$ = 16.6 Hz). $^{13}$C NMR (100 MHz, $CDCl_3$, $\delta$ ppm): 183.2, 158.3, 155.4, 154.7, 150.8, 148.9, 146.5, 146.0, 145.5, 142.7, 141.6, 139.7, 137.3, 136.2, 135.3, 132.4, 131.6, 131.3, 130.6, 129.0, 128.1, 121.8, 117.4, 68.4, 53.7, 32.0, 31.9, 31.8, .31.2, 29.6, 29.5, 29.2, 28.7, 26.3, 22.9, 22.8, 14.4.

**Synthesis of compound 8c.** Compound **8c** was synthesized similarly as described for compound **8a**. Deep red solid, yield 55% (103 mg). $^1$H NMR (400 MHz, $CDCl_3$, $\delta$ ppm): 10.15 (s, 1H), 7.98 (s, 1H), 7.90 (s, 1H), 7.76-7.74 (m, 4H), 7.41-7.32 (m, 8H), 7.13 (d, 4H, $J$ = 8.6 Hz), 6.98 (d, 2H, $J$ = 8.2 Hz), 6.86 (d, 4H, $J$ = 8.5 Hz), 3.88 (t, 4H, $J$ = 6.5 Hz), 2.97 (t, 2H, $J$ = 7.8 Hz), 2.69 (t, 2H, $J$ = 7.9 Hz), 1.70 (m, 8H), 1.45-1.11 (m, 32H), 0.82 (t, 12H, $J$ = 5.6 Hz). $^{19}$F NMR (376 MHz, $CDCl_3$, $\delta$ ppm): -126.26, -128.32. $^{13}$C NMR (100 MHz, $CDCl_3$, $\delta$ ppm):183.2, 160.3, 157.1, 155.5, 154.8, 153.2, 152.2, 152.0, 151.2, 149.7, 149.0, 148.3, 147.5, 146.8, 145.6, 145.0, 143.5, 143.3, 142.2, 141.3, 140.7, 139.9, 138.1, 137.7, 134.0, 133.9, 130.2, 115.4, 98.1, 68.5, 53.7, 32.1, 31.9, 31.8, 31.2, 29.6, 29.5, 29.3, 28.7, 26.3, 22.9, 22.8, 14.4.

**Synthesis of sensitizer FNE54.** Under nitrogen atmosphere, a mixture of compound **8a** (149 mg, 0.15 mmol) and cyanoacetic acid (38 mg, 0.45 mol) in acetonitrile (10 mL) was refluxed in the presence of piperidine (0.1 mL) for 10 h. After cooling to room temperature, poured into water and extracted with DCM, the combined organic solution was washed with water and sodium chloride solution and dried over anhydrous sodium sulfate. After removal of the solvent, the residue was purified by flash column chromatography (silica gel, DCM/MeOH = 10/1). Black solid, yield 60% (100 mg). $^1$H NMR (400 MHz, THF-$d_8$, $\delta$ ppm): 9.03 (d, 1H, $J$ = 12.6 Hz), 8.47 (s, 1H), 8.38 (s, 1H), 8.32 (s, 1H), 8.00 (s, 1H), 7.92 (s, 1H), 7.32 (d, 2H, $J$ = 7.6 Hz), 7.07 (d, 4H, $J$ = 8.4 Hz), 6.93 (d, 2H, $J$ = 7.9 Hz), 6.86 (d, 4H, $J$ = 8.9 Hz), 3.95 (t, 4H, $J$ = 6.3 Hz), 2.91 (t, 2H, $J$ = 8.0 Hz), 2.76 (t, 2H, $J$ = 7.6 Hz), 2.65-2.43 (m, 8H), 1.36-1.29 (m, 32H), 0.9 (t, 12H, $J$ = 7.6 Hz). $^{13}$C NMR (100 MHz, THF-$d_8$, $\delta$ ppm): 158.1, 155.2, 154.6, 150.5, 148.4, 146.3, 145.8, 145.3, 142.5, 141.4, 139.5, 137, 136, 135.1, 132.3, 132.2, 131.6, 131.4, 131.1, 130.3, 129.5, 128.8, 128.3, 127.9, 121.6, 121.1, 117.1, 69.8, 33.9, 33.8, 33.7, 33.5, 33.1, 31.7, 31.5, 31.4, 31.1, 30.7, 28.2, 26.8, 26.6, 26.4, 26.2, 26.0, 24.6, 24.5, 15.5. HRMS: *m/z* calcd for $C_{66}H_{80}N_4O_4S_2$, 1056.5621; found 1056.5623.

**Synthesis of sensitizer FNE55.** Compound **FNE55** was synthesized similarly as described for **FNE54**. Black solid, yield 65% (60 mg). $^1$H NMR (400 MHz, DMSO-$d_6$, $\delta$ ppm): 9.07 (d, 1H, $J$ = 3.0 Hz), 8.24 (s, 1H), 7.82 (d, 1H, $J$ = 7.4 Hz), 7.32 (d, 1H, $J$ = 8.5 Hz), 7.06 (d, 2H, $J$ = 8.9 Hz), 6.91 (d, 2H, $J$ = 8.9 Hz), 6.83 (d, 1H, $J$ = 8.5 Hz), 3.89 (t, 4H, $J$ = 6.5 Hz,), 2.99 (t, 2H, $J$ = 7.8 Hz), 2.69 (t, 2H, $J$ = 7.9 Hz), 1.70 (m, 8H), 1.45-1.11 (m, 32H), 0.82 (t, 12H, $J$ = 5.6 Hz). $^{19}$F NMR (376 MHz, DMSO-$d_6$, $\delta$ ppm): -128.30 (d, $J$ = 19.9 Hz), -129.96 (d, $J$ = 19.9 Hz). $^{13}$C NMR (100 MHz, $CDCl_3$, $\delta$ ppm): 168.8, 155.7, 151.5, 149.7, 148.7, 148.1, 147.4, 144.3, 142.6, 140.7, 137.3, 136.4, 135.0, 134.2, 131.3, 129.6, 126.9, 126.3, 120.0, 119.2, 115.4, 102.2, 66.4, 34.3, 32.1, 31.9, 31.1, 30.9, 30.5, 29.9, 29.6, 29.5, 29.0, 28.7, 28.4, 22.9, 21.3, 14.3. HRMS: *m/z* calcd for $C_{66}H_{78}F_2N_4O_4S_2$, 1092.5433; found 1092.5419.

**Synthesis of sensitizer FNE56.** Compound **FNE56** was synthesized similarly as described for **FNE54**. Black solid, yield 50% (54 mg). $^1$H NMR (400 MHz, DMSO-$d_6$, $\delta$ ppm): 8.22 (s, 1H), 7.97 (s, 1H), 7.89 (s, 1H), 7.75 (d, 2H, $J$ = 6.7 Hz), 7.68 (s, 2H), 7.40 (d, 6H, $J$ = 7.7 Hz), 7.31 (d, 2H, $J$ = 9.0 Hz), 7.08 (d, 4H, $J$ = 8.8 Hz), 6.92 (d, 4H, $J$ = 8.8 Hz), 6.83 (d, 2H, $J$ = 8.5 Hz) 3.90 (t, 4H, $J$ = 6.5 Hz), 3.02 (t, 2H, $J$ = 7.8 Hz), 2.79 (t, 2H, $J$ = 7.9 Hz), 1.70 (m, 8H), 1.45-1.11 (m, 32H), 0.82 (t, 12H, $J$ = 5.6 Hz). $^{19}$F NMR (376 MHz, DMSO-$d_6$, $\delta$ ppm): -128.62 (d, $J$ = 18.6 Hz), -130.47 (d, $J$ = 18.6 Hz). $^{13}$C NMR (100 MHz, $CDCl_3$, $\delta$ ppm): 173.4, 155.8, 151.2, 148.2, 144.1, 140.7, 138.4, 137.5, 134.5, 134.3, 130.9, 130.0, 128.3, 127.0, 125.2, 121.9, 119.9, 115.5, 66.5, 32.1, 32.0, 31.2, 29.9, 29.6,



 

29.5, 26.3, 22.9, 14.4, 14.3. HRMS: *m/z* calcd for $C_{78}H_{86}F_2N_4O_4S_2$, 1244.6059; found, 1244.6028.

**Characterizations.** $^1$H NMR (400 MHz), $^{19}$F NMR (376 MHz), and $^{13}$C NMR (100 MHz) spectra were measured on a Varian Mercury Plus-400 spectrometer. The splitting patterns are designated as follows: s (singlet); d (doublet); t (triplet); q (quartet); m (multiplet). UV-vis absorption spectra of dye solutions and dye-loaded films were recorded with a Shimadzu UV-2550PC spectrophotometer. The film thickness was measured by a surface profiler (Veeco Dektak 150). Cyclic voltammetry (CV) measurements were performed with a CHI660E electrochemical workstation using a typical three-electrode electrochemical cell in a solution of tetrabutylammonium hexafluorophosphate (0.1 M) in water-free acetonitrile with a scan rate of 50 mV $s^{-1}$ at room temperature under argon. Dye adsorbed $TiO_2$ film (0.25 $cm^2$) on FTO glass was used as the working electrode, a Pt wire as the counter electrode, and an $Ag/Ag^+$ electrode as the reference electrode. The potential of the reference electrode was calibrated by ferrocene, and all potentials mentioned in this work are against normal hydrogen electrode (NHE).

**DSSC Fabrication and Photovoltaic Measurements.** The quasi-solid-state DSSCs based on the resulting sensitizers (0.3 mM) with coadsorption of deoxycholic acid (10 mM) were constructed according to our previously reported method.[15m] The gel electrolyte contains 0.1 M LiI, 0.1 M $I_2$, 0 or 0.1 M *tert*-butylpyridine, 0.6 M 1,2-dimethyl-3-propylimidazolium iodide, and 5wt% poly(vinylidenefluoride-*co*-hexafluoropropylene) in 3-methoxypropionitrile. The active area is 0.25 $cm^2$. The current density-voltage (*J-V*) characteristics of the DSSCs were measured by recording *J-V* curves using a Keithley 2400 source meter under the illumination of AM1.5G simulated solar light coming from a solar simulator (Oriel-91193 equipped with a 1000 W Xe lamp and an AM1.5G filter). The incident light intensity was calibrated with a standard silicon solar cell (Newport 91150). The electron lifetimes were measured with intensity modulated photovoltage spectroscopy (IMVS), whereas charge densities at open-circuit were measured using charge extraction technique. IMVS analysis and charge extraction were carried out on an electrochemical workstation (Zahner XPOT, Germany), which includes a white light emitting diode and corresponding control system. The intensity modulated spectra were measured at room temperature with light intensity ranging from 20 to 120 W $m^{-2}$, in modulation frequency ranging from 0.1 Hz to 10 kHz, and with modulation amplitude less than 5% of the light intensity. The electron lifetime was calculated by equation $\tau=1/2\pi f_{min}$, where $f_{min}$ is the frequency at the top of the semicircle ($f_{min}$) in IMVS. Action spectra of the incident monochromatic photon-to-electron conversion efficiency (IPCE) for the solar cells were obtained with an Oriel-74125 system (Oriel Instruments). The intensity of monochromatic light was measured with a Si detector (Oriel-71640).

## Results and Discussion

### Synthesis of Sensitizers

The synthetic route to sensitizers **FNE55**, and **FNE56** is depicted in Scheme 1, which starts from 5,6-difluoro-4,7-diiodobenzo[*c*][1,2,5]thiadiazole (**1**).[16] Via a Stille coupling[18] with tributyl(4-hexylthien-2-yl)stannane, intermediate compound 5,6-difluoro-4,7-bis(4-hexylthien-2-yl)benzo[c]-[1,2,5]thiadiazole (**2**) was provided. Then the thiadiazole ring was reduced to two amino groups and further converted to pyrazine ring by ring-closure condensation with oxalaldehyde and benzyl to produce the key spacer **4b** and **4c**,respectively. After refluxing with a Vilsmeier reagent,[19] the corresponding monoaldehyde-substituted derivatives **6b** and **6c** were synthesized and then converted to bromides **7b** and **7c**, respectively, by bromination with NBS. Electron donor, triarylamine, was attached via Suzuki coupling[20] with *N*,*N*-bis(4-octyloxyphenyl)-(4-(4,4,5,5-tetramethyl-1,3,2-dioxaborolan-2-yl)phenyl)aniline, which produced the precursors **8b** and **8c**. In the last step, the obtained precursors were converted to the corresponding sensitizers **FNE55** and **FNE56**, respectively, by Knoevenagel condensation[21] with cyanoacetic acid through refluxing acetonitrile in the presence of piperidine. Correspondingly, reference sensitizer **FNE54** was synthesized similarly from non-fluoro substituted starting material 5,8-dibromoquinoxaline (**5**). All the target sensitizers were characterized by $^1$H, $^{19}$F, $^{13}$C NMR spectroscopy, and HRMS spectroscopy, and were found to be consistent with the proposed structures.

### Photophysical Properties

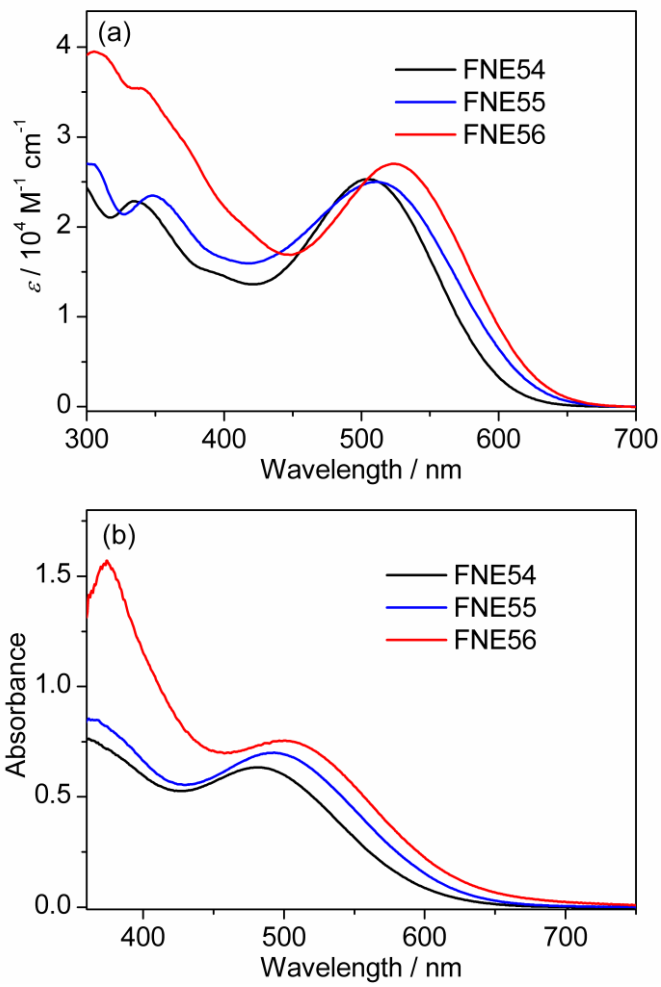


**Fig. 2** UV-vis absorption spectra of sensitizers **FNE54**, **FNE55**, and **FNE56** (a) in toluene solutions and (b) on $TiO_2$ films.

The UV-vis absorption spectra (Fig. 2) of the target sensitizers were recorded in toluene solutions (~$10^{-5}$ M) and on $TiO_2$ films (~3 μm). The corresponding data are summarized in Table 1. It can be found that all the sensitizers exhibit two distinct absorption bands. The

absorption band in the ultraviolet region corresponds to the π–π* electron transitions of the conjugated backbone, while the other one in the visible region is assigned to the intramolecular charge transfer (ICT) from the electron-donating moiety to the electron-withdrawing moiety. As shown in Fig. 2a, sensitizer **FNE54** displays the maximum absorption wavelength at 504 nm in toluene solution. Upon the incorporation of two fluorine atoms on the quinoxaline unit, sensitizer **FNE55** displays a slightly bathochromically shifted absorption maximum at 511 nm. However, it should be noted that the ICT band of sensitizer **FNE55** is much broader and the absorption on-set is bathochromically shifted by more than 20 nm as compared with that for sensitizer **FNE54**. This is obviously due to the introduced two fluorines on the quinoxaline unit, which strengthen the ICT interactions in sensitizer **FNE55** and result in the reduced band gap. Moreover, when two phenyl rings are incorporated at the 2,3-postion of quinoxaline unit, the absorption maximum further bathochromically shifts to 525 nm, which is owning to the extended π-conjugation in the spacer part upon the introduction of two phenyl rings.

The UV-vis absorption spectra for the dye-loaded $TiO_2$ films are shown in Fig. 2b. The absorption maximum wavelength bathochromically shifts from 480 nm for **FNE54** to 492 nm for **FNE55**, and further to 501 nm for **FNE56**, which display the same trend for the absorption maxima as those for their absorption spectra in toluene solutions. Furthermore, in comparison to the maximum absorption band of the sensitizers in toluene solutions, all the sensitizers display a hypsochromically shifted absorption maximum around 20 nm on $TiO_2$ films. This phenomenon has been observed for most of organic sensitizers and is due to the deprotonation of cyanoacrylic acid group.[12b, 14, 15h, 15m] However, unlike most reported D-π-A system, where the hypsochromic shift for absorption maximum from the solution to the dye loaded $TiO_2$ film is much larger, the slight hypsochromic shift in this case is obviously due to the weakened deprotonation effect caused by the additional quinoxaline acceptor. After anchoring sensitizers onto $TiO_2$ surface, although the anchor group was deprotonated, the ICT from the electron donor to the inserted quinoxaline moiety was not weakened significantly and therefore only slight hypsochromic shift could be observed. This phenomenon is similar to previously reported D-A'-π-A featured organic dyes.[11]

**Table 1.** UV-vis absorption and electrochemical properties of sensitizers **FNE54**, **FNE55**, and **FNE56**.

| Dye | Absorption | | | HOMO[b] | $E_g$ | LUMO[b] |
|---|---|---|---|---|---|---|
| | $\lambda_{max}$[a] nm | $\varepsilon$[a] $M^{-1}$ $cm^{-1}$ | $\lambda_{max}$ on $TiO_2$ nm | V | eV | V |
| **FNE54** | 504 | $2.5\times10^4$ | 480 | 0.96 | 2.03 | -1.07 |
| **FNE55** | 511 | $2.5\times10^4$ | 492 | 1.00 | 1.98 | -0.98 |
| **FNE56** | 525 | $2.7\times10^4$ | 501 | 1.01 | 1.92 | -0.91 |

[a] Absorption peaks ($\lambda_{max}$) and molar extinction coefficients ($\varepsilon$) were measured in toluene solutions (~$10^{-5}$ M). [b] The potentials (*vs.* NHE) were calibrated with ferrocene.

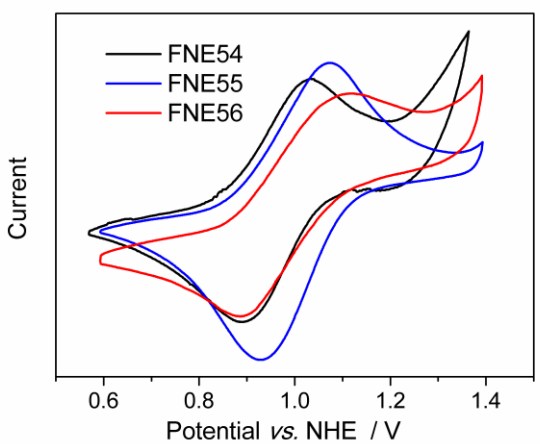


**Fig. 3** Cyclic voltammograms of the dye-loaded $TiO_2$ films.

### Electrochemical Properties.

To determine the oxidation potential of the organic sensitizers and thermodynamically evaluate the possibility of sensitizer regeneration, cyclic voltammograms (CV) was carried out carried out in a typical three-electrode electrochemical cell with $TiO_2$ films stained with sensitizer as the working electrode in a solution of tetrabutylammonium hexafluorophosphate (0.1 M) in water-free acetonitrile with a scan rate of 50 mV $s^{-1}$. As shown in Fig. 3 and Table 1, the HOMO level, corresponding to the first half-wave oxidation potential, is determined to be 0.96, 1.00, and 1.01 V (*vs.* normal hedrogen electrode, NHE) for sensitizers **FNE54**, **FNE55**, and **FNE56**, respectively. The close HOMO values for the three dyes are not difficult to be understood since they originate from the oxidation of the same triarylamine moiety. These values are much more positive than the redox potential for $I^-/I_3^-$ redox couples (~0.4 V *vs.* NHE), indicating that the reduction of the oxidized dyes with $I^-$ ions is thermodynamically feasible. Then the LUMO energy level was estimated from equation (1),

$$\text{LUMO} = \text{HOMO} - \Delta E \qquad (1)$$

where $\Delta E$ is the energy gap between the HOMO and LUMO levels and derived from the wavelength at 10% maximum absorption intensity for the dye-loaded $TiO_2$ film.[22] Correspondingly, the LUMO levels for sensitizers **FNE54**, **FNE55**, and **FNE56**, are calculated to be -1.07, -0.98, and -0.91 V (*vs.* NHE), respectively. This suggests that the driving force of the electron injection from their excited states for all the sensitizers is still enough after incorporation of fluorines into the molecular backbone of the organic sensitizers.

### Theoretical Approach

To investigate the geometrical structures and electronic properties of the organic dye isomers, density functional calculations were conducted with the Gaussian 03 program using B3LYP method and 6-31G* basis set.[23] As shown in Fig. 4, for all the resulting dyes, the HOMO extensively distributes over the π-system of the donor part, while the LUMO delocalizes over the A-π-A moiety with large composition on the anchoring group, where the electron is close to the $TiO_2$ semiconductor. Moreover, the distributions of HOMO and



 

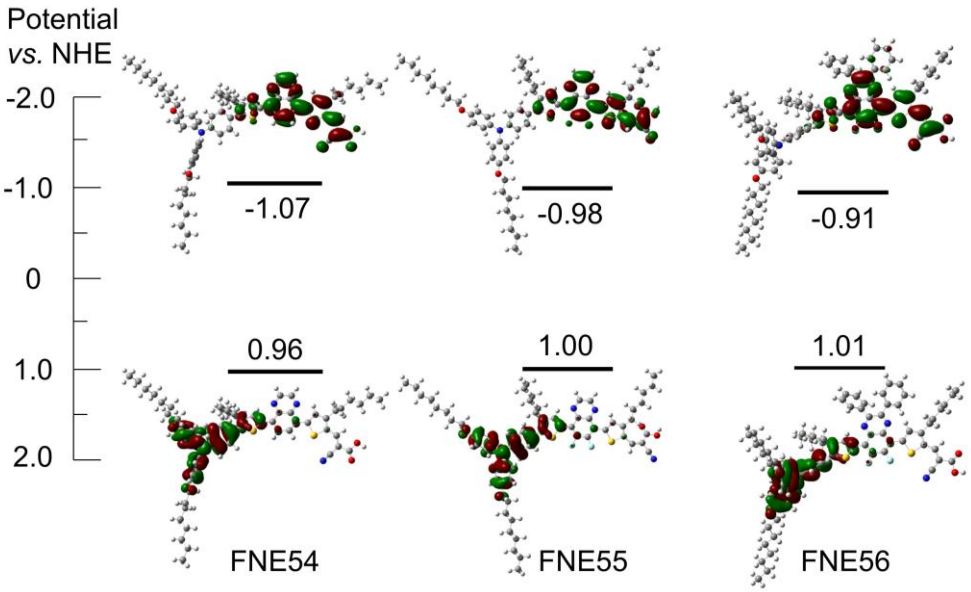


**Fig. 4** Calculated frontier molecular orbitals and experimental energy level diagram of sensitizers **FNE54**, **FNE55**, and **FNE56**.

**Table 1** Photovoltaic performance of the quasi-solid-state DSSCs based on the resulting sensitizers.

| Dye | $C_{TBP}$ M | $V_{oc}$ mV | $J_{sc}$ mA cm$^{-2}$ | *FF* | $\eta$ % |
|---|---|---|---|---|---|
| **FNE54** | 0 | 593 | 13.16 | 0.65 | 5.1 |
| | 0.1 | 626 | 13.88 | 0.69 | 6.0 |
| **FNE55** | 0 | 597 | 14.60 | 0.68 | 5.9 |
| | 0.1 | 634 | 15.57 | 0.69 | 6.8 |
| **FNE56** | 0 | 664 | 15.08 | 0.67 | 6.7 |
| | 0.1 | 676 | 17.76 | 0.68 | 8.2 |

LUMO are overlapped within the quinoxaline unit and the neighboured thiophene ring, indicating that the photo-excited electrons could be successively transferred from the donor moiety to the quinoxaline unit, then transferred to the cyanoacetic acid subunit, and finally into $TiO_2$.

### Solar Cell Performance

The quasi-solid-state DSSCs based on the resulting sensitizers (0.3 mM) with coadsorbtion of deoxycholic acid (10 mM) were constructed using a gel electrolyte containing 0.1 M LiI, 0.1 M $I_2$, 0.6 M 1,2-dimethyl-3-propylimidazolium iodide, and 5wt% poly(vinylidenefluoride-*co*-hexafluoropropylene) in 3-methoxypropionitrile. To evaluate the influence of the introduced fluorines on the DSSC performance, the quasi-solid-state DSSCs were fabricated with or without 4-*tert*-butylpyridine (TBP, 0.1 M) as additive in the gel electrolyte. The solar-to-electricity conversion efficiencies of DSSCs were measured by recording the photocurrent density-voltage (*J*-*V*) characteristics at simulated AM1.5G solar light (100 mW cm$^{-2}$). As shown in Table 1, all the quasi-solid-state DSSCs based on the electrolyte with TBP display higher $J_{sc}$ and $V_{oc}$ values as compared with those for the DSSCs based on the electrolyte without TBP. The increased $J_{sc}$ values are probably due to the reduced charge recombination rate and decreased current loss caused by the coating of TBP on $TiO_2$ nanoparticles. While the higher $V_{oc}$ values are owning to the negative shift of conduction band of $TiO_2$ caused by the adsorption of TBP on $TiO_2$ surface, which enlarges the energy level difference between the Fermi level of $TiO_2$ and the redox potential under light irradiation.[24] These results suggests that upon the incorporation of fluorines in the organic dye molecules, the offset between the LUMO level of the organic sensitizer and the conduction band edge of titania semiconductor is still enough to ensure a fast and efficient electron injection. Consequently, the highest performance was achieved for **FNE56** based quasi-solid-state DSSC, which provided a $J_{sc}$ of 17.76 mA cm$^{-2}$, a $V_{oc}$ of 0.676 V, and a *FF* of 0.68, respectively, corresponding a $\eta$ of 8.2% (Fig. 5), which is one of the highest values for organic dye based quasi-solid-state DSSCs ever reported so far.

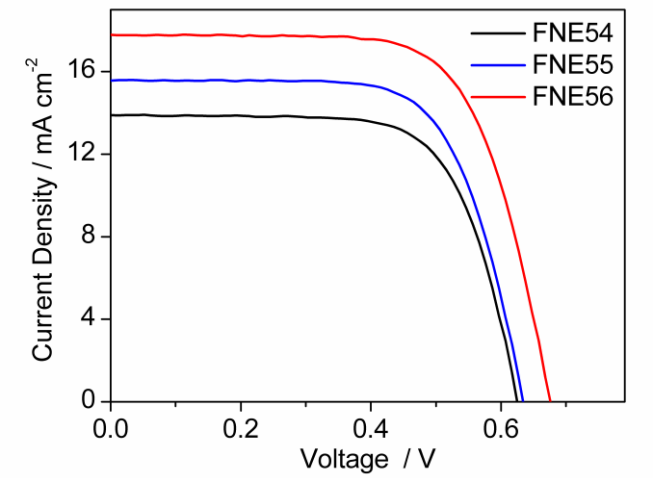


**Fig. 5** *J* – *V* curves for the quasi-solid-state DSSCs with TBP in the electrolyte.

Action spectra of the incident photon-to-electron conversion efficiencies (IPCE) as a function of incident wavelength for the quasi-solid-state DSSCs were recorded and shown in Fig. 6. All the quasi-solid-state DSSCs based on the resulting sensitizers display

the highest IPCE values of over 80%. However, the IPCE spectrum for the DSSCs based on **FNE55** and **FNE56**, respectively, is much broader than that for **FNE54**, which is in good agreement with their absorption spectra (Fig. 2) and beneficial to light-harvesting and photocurrent generation. With an extended IPCE response, the quasi-solid-state DSSCs based on sensitizers **FNE55** and **FNE56** containing fluorine provide higher photogenerated currents as compared with **FNE54** based DSSC.

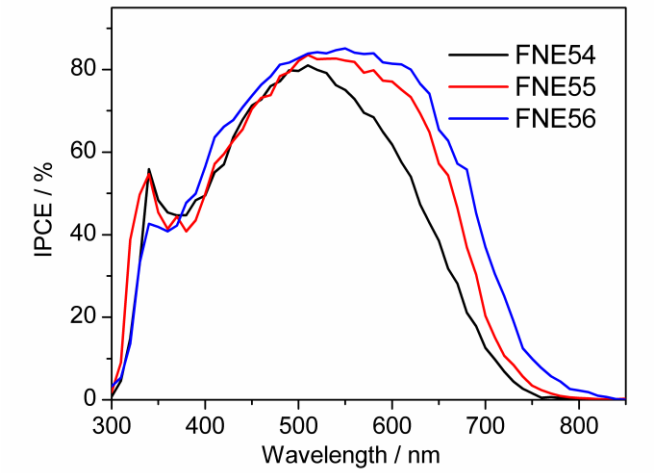


**Fig. 6** IPCE spectra for the quasi-solid-state DSSCs with TBP in the electrolyte.

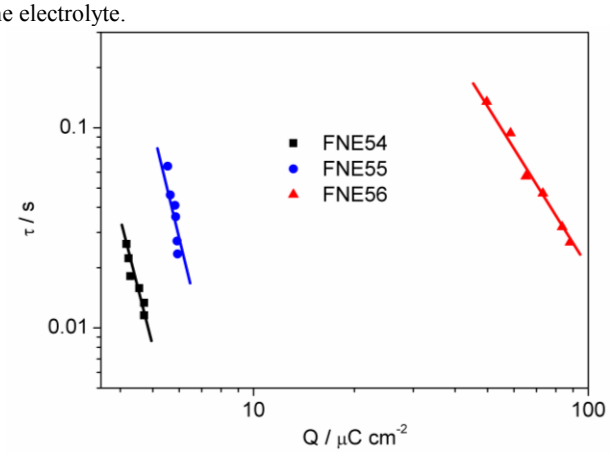


**Fig. 7** Electron lifetime as a function of electron density at open circuit for the quasi-solid-state DSSCs based on sensitizers **FNE54**, **FNE55**, and **FNE56**.

To explain the $V_{oc}$ difference among the quasi-solid-state DSSCs, the electron lifetime against charge density for the DSSCs was investigated since $V_{oc}$ is related to the conduction band position of $TiO_2$ and the charge recombination rate in DSSCs.[25] The electron lifetime was calculated by equation (2):[26]

$$\tau = (2\pi f_{min})^{-1} \qquad (2)$$

where $f_{min}$ is the frequency at the top of the semicircle ($f_{min}$) measured by IMVS. Fig. 7 shows the electron lifetime as a function of charge density at open circuit. It can be found that at the same charge density, **FNE56** based quasi-solid-state DSSC displays the longest electron lifetime probably due to the two phenyl rings substituted at 2,3-positions of quinoxaline unit which have weakened the intermolecular interactions and therefore suppressed the charge recombination between electrons in $TiO_2$ film and electron acceptors, as reported by Zhu et. al.[15e] The reduced charge recombination rate constant reduces electron loss at open circuit. Since the conduction band positions are generally identical for the DSSCs based on sensitizers with similar chemical structures, when more electrons are accumulated in $TiO_2$, the Fermi level moves upward and therefore $V_{oc}$ gets larger.

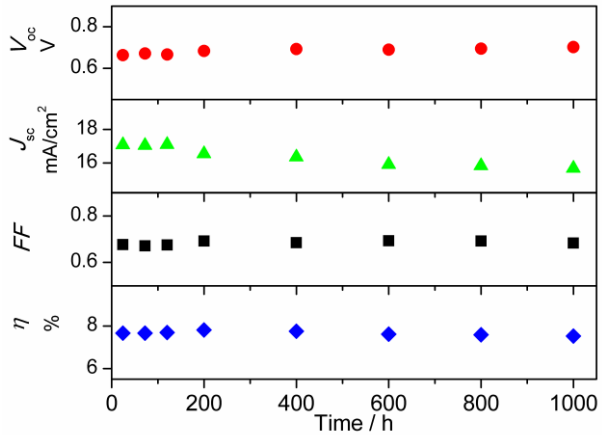


**Fig. 8** Evolutions of photovoltaic performance parameters for **FNE56** based quasi-solid-state DSSC during one sun soaking.

Long-term stability is considered as an important requirement for evaluating the practical application of the DSSC in the future. Therefore, the stability of the quasi-solid-state DSSCs based on the resulting sensitizers was recorded over a period of 1000 h under one sun soaking. Fig. 8 displays the photovoltaic performance parameters of sensitizer **FNE56** based quasi-solid-state DSSC under sunlight soaking. It can be found that the $J_{sc}$, $V_{oc}$, and $FF$ parameters slightly change during the DSSC operation. This is probably due to the further infiltration of the quasi-solid-state electrolyte in the mesoporous $TiO_2$ films. The adsorption of TBP on $TiO_2$ surface will negative shift of conduction band of $TiO_2$,[24] which lowers down the driving force for the electron injection but enlarges the energy gap between the Fermi level of $TiO_2$ and the redox potential of the electrolyte. As a result, the $J_{sc}$ drops but $V_{oc}$ increases with sunlight socking time. Most importantly, the power conversion efficiency remained 98% of the initial value after 1000 h of one sun soaking, which indicates that sensitizer **FNE56** is sufficiently stable for DSSC application.

## Conclusions

In summary, two organic sensitizers possessing fluorinated quinoxaline moiety have been designed and successfully synthesized. The incorporation of fluorine in the organic dye molecules successfully lowers down the sensitizer band gap, meanwhile maintaining enough driving force for efficient electron injection. Consequently, **FNE56** based quasi-solid-state DSSC displays a highest $\eta$ of 8.2%, which exhibits good long-term stability after continuous sunlight soaking for 1000 h.

## Acknowledgements

This work was financially supported by the National Basic Research Program of China (2011CB933302), the National Natural Science Foundation of China (51273045), NCET-12-0122, STCSM (12JC1401500), Shanghai Leading Academic Discipline Project (B108), and Jiangsu Major Program (BY2010147).

## Notes and references

Lab of Advanced Materials & Department of Chemistry, Fudan University, Shanghai 200438, P. R. China. E-mail: zhougang@fudan.edu.cn

† These authors contributed equally to this work.

1 O'Regan and M. Grätzel, *Nature*, 1991, **353**, 737.
2 (a) M. K. Nazeeruddin, A. Kay, I. Rodicio, R. Humphry-Baker, E. Mueller, P. Liska, N. Vlachopoulos and M. Grätzel, *J. Am. Chem. Soc.*, 1993, **115**, 6382; (b) M. K. Nazeeruddin, P. Péchy, T. Renouard, S. M. Zakeeruddin, R. Humphry-Baker, P. Comte, P. Liska, L. Cevey, E. Costa, V. Shklover, L. Spiccia, G. B. Deacon, C. A. Bignozzi and M. Grätzel. *J. Am. Chem. Soc.*, 2001, **123**, 1613; (c) M. K. Nazeeruddin, F. D. Angelis, S. Fantacci, A. Selloni, G. Viscardi, P. Liska, S. Ito, B. Takeru and M. Grätzel, *J. Am. Chem. Soc.*, 2005, **127**, 16835; (d) A. Yella, H. W. Lee, H. N. Tsao, C. Yi, A. K. Chandiran, M. K. Nazeeruddin, E. W. G. Diau, C. Y. Yeh, S. M. Zakeeruddin and M. Grätzel, *Science*, 2011, **334**, 629; (e) W.-Q. Wu, H.-L. Feng, H.-S. Rao, Y.-F. Xu, D.-B. Kuang and C.-Y. Su, *Nat. Commun.*, 2014, **5**, 3968; (e) H. Zhou, Q. Chen, G. Li, S. Luo, T. Song, H.-S. Duan, Z. Hong, J. You, Y. Liu and Y. Yang, *Science*, 2014, **345**, 542.
3 S. Mathew, A. Yella, P. Gao, R. Humphry-Baker, F.E. Curchod, N. Ashari-Astani, I. Tavernelli, U. Rothlisberger, M. K. Nazeeruddin and M. Grätzel, *Nature Chem*., 2014, **6**, 242.
4 P. Wang, S. M. Zakeeruddin, J. E. Moser, M. K. Nazeeruddin, T. Sekiguchi and M. Grätzel, *Nat. Mater.*, 2003, **2**, 402.
5 M. Grätzel, *J. Photoch. Photobio. A*, 2004, **164**, 3.
6 Y. Wang, S. R. Parkin, J. Gierschner and M. D. Watson, *Org. Lett.*, 2008, **10**, 3307.
7 W. Lu, J. Kuwabara, T. Iijima, H. Higashimura, H. Hayashi and T. Kanbara, *Macromolecules*, 2012, **45**, 4128.
8 T. Lei, J.-H. Dou, Z.-J. Ma, C.-H. Yao, C.-J. Liu, J.-Y. Wang and J. Pei, *J. Am. Chem. Soc.*, 2012, **134**, 20025.
9 (a) J. Min, Z.-G. Zhang, S. Zhang and Y. Li, *Chem. Mater*., 2012, **24**, 3247. (b) H.-C. Chen, Y.-H. Chen, C.-C. Liu, Y.-C. Chien, S.-W. Chou, and P.-T. Chou, *Chem. Mater*., 2012, **24**, 4766. (c) H.-C. Chen, Y.-H. Chen, C.-H. Liu, Y.-H. Hsu, Y.-C. Chien, W.-T. Chuang, C.-Y. Cheng, C.-L. Liu, S.-W. Chou, S.-H. Tung and P.-T. Chou, *Polym. Chem.*, 2013, *4*, 3411.
10 (a) Y.-S. Yen, C.-T. Lee, C.-Y. Hsu, H.-H. Chou,Y.-C. Chen and J. T. Lin, *Chem. Asian J*., 2013, **8**, 809; (b) N. Cho, J. Han, K. Song, M.-S. Kang, M.-J. Jun, Y. Kang and J. Ko, *Tetrahedron*, 2014, **70**, 427; (c) Y. Wang, X. Xin, Y. Lu, T. Xiao, X. Xu, N. Zhao, X. Hu, B. S. Ong and S. C. Ng, *Macromolecules*, 2013, **46**, 9587; (d) D. Dang, W. Chen, R. Yang, W. Zhu, W. Mammo and E. Wang, *Chem. Commun.*, 2013, **49**, 9335; (e) J.-H. Kim, C. E. Song, H. U. Kim, A. C. Grimsdale, S.-J. Moon, W. S. Shin, S. K. Choi and D.-H. Hwang, *Chem. Mater*., 2013, **25**, 2722; (f) S. Paek, N. Cho, K. Song, M.-J. Jun, J. K. Lee and J. Ko, *J. Phys. Chem. C*, 2012, **116**, 23205; (g) D.-Y. Chen, Y.-Y. Hsu, H.-C. Hsu, B.-S. Chen, Y.-Tsung. Lee, H. Fu, M.-W. Chung, S.-H. Liu, H.-C. Chen, Y. Chi and P.-T. Chou, *Chem. Commun*., 2010, **46**, 5256; (h) B.-S. Chen, D.-Y. Chen, C.-L. Chen, C.-W. Hsu, H.-C. Hsu, K.-L. Wu, S.-H. Liu, P.-T. Chou and Y. Chi, *J. Mater. Chem.*, 2011, **21**, 1937; (i) X. Kang, J. Zhang, D. O'Neil, A. J. Rojas, W. Chen, P. Szymanski, S. R. Marder and M. A. El-Sayed, *Chem. Mater.*, 2014, **26**, 4486
11 Y. Wu and W. Zhu, *Chem. Soc. Rev.*, 2013, **42**, 2039.
12 (a) M. Velusamy, K. R. J. Thomas, J. T. Lin, Y. C. Hsu and K. C. Ho, *Org.Lett*., 2005, **7**, 1899; (b) W. H. Zhu, Y. Z. Wu, S. T. Wang, W. Q. Li, X. Li, J. Chen, Z. S. Wang and H. Tian, *Adv. Funct. Mater*., 2011, **21**, 756; (c) Y. Z. Wu, X. Zhang, W. Q. Li, Z. S. Wang, H. Tian and W. H. Zhu, *Adv. Energy Mater*., 2012, **2**, 149; (d) D. H. Lee, M. J. Lee, H. M. Song, B. J. Song, K. D. Seo, M. Pastore, C. Anselmi, S. Fantacci, F. De Angelis, M. K. Nazeeruddin, M. Grätzel and H. K. Kim, *Dyes Pigm.*, 2011, **91**, 192; (e) J. Kim, H. Choi, J. Lee, M. Kang, K. Song, S. O. Kang and J. Ko, *J. Mater. Chem*., 2008, **18**, 5223; (f) Z. M. Tang, T. Lei, K. J. Jiang, Y. L. Song and J. Pei, *Chem. -Asian J*., 2010, **5**, 1911; (g) S. Kim, H. Lim, K. Kim, C. Kim, T. Y. Kang, M. J. Ko and N. G. Park, *IEEE J. Sel. Top. Quantum Electron*., 2010, **16**, 1627; (h) S. Haid, M. Marszalek, A. Mishra, M. Wielopolski, J. Teuscher, J. Moser, R. Humphry-Baker, S. M. Zakeeruddin, M. Grätzel and P. Bäuerle, *Adv. Funct. Mater*., 2012, **22**, 1291; (i) Y. Z. Wu, M. Marszalek, S. M. Zakeeruddin, Q. Zhang, H. Tian, M. Grätzel and W. H. Zhu, *Energy Environ. Sci*., 2012, **5**, 8261; (j) Q. Feng, X. Jia, G. Zhou, Z.-S. Wang, *Chem. Commun*., 2013, **49**, 7445; (k) S. Cai, X. Hu, Z. Zhang, J. Su, X. Li, A Islam, L. Han, H. Tian, *J. Mater. Chem. A*, 2013, **1**, 4763; (l) A Yella, C.-L. Mai, S. M. Zakeeruddin, S.-N. Chang, C.-H. Hsieh, C.-Y. Yeh, M. Grätzel, *Angew. Chem. Int. Ed*., 2014, **53**, 2973.
13 (a) S. Y. Qu, W. J. Wu, J. L. Hua, C. Kong, Y. T. Long and H. Tian, *J. Phys. Chem. C*, 2010, **114**, 1343; (b) S. Y. Qu, B. Wang, F. L. Guo, J. Li, W. J. Wu, C. Kong, Y. T. Long and J. L. Hua, *Dyes Pigm*., 2012, **92**, 1384; (c) S. Y. Qu, C. J. Qin, A. Islam, Y. Z. Wu, W. H. Zhu, J. L. Hua, H. Tian and L. Y. Han, *Chem. Commun*., 2012, **48**, 6972; (d) J. Warnan, L. Favereau, Y. Pellegrin, E. Blart, D. Jacquemin and F. Odobel, *J. Photochem. Photobiol. A*, 2011, **226**, 9; (e) F. L. Guo, S. Y. Qu, W. J. Wu, J. Li, W. J. Ying and J. L. Hua, *Synth. Met*., 2010, **160**, 1767; (f) L. Favereau, J. Warnan, F. B. Anne, Y. Jacquemin, F. Odobel, *J. Mater. Chem. A*, 2013, **1**, 7572; (g) F. Zhang, K.-J. Jiang, J.-H. Huang, C.-C. Yu, S.-G. Li, M.-G. Chen, L.-M. Yang and Y.-L. Song, *J. Mater. Chem. A*, 2013, **1**, 4858.
14 W. Ying, J. Yang, M. Wielopolski, T. Moehl, J.-E. Moser, P. Comte, J. Hua, S. M. Zakeeruddin, H. Tian and M. Grätzel, *Chem. Sci*., 2014, **5**, 206.
15 (a) D. W. Chang, H. J. Lee, J. H. Kim, S. Y. Park, S.-M. Park, L. Dai and J.-B. Baek, *Org.Lett*., 2011, **13**, 3880; (b) S.-R. Li, C.-P. Lee, H.-T. Kuo, K.-C. Ho and S.-S. Sun, *Chem. Eur. J*., 2012, **18**, 12085; (c) J. Shi, J. Chen, Z. Chai, H. Wang, R. Tang, K. Fan, M. Wu, H. Han, J. Qin, T. Peng, Q. Li and Z. Li, *J. Mater. Chem*., 2012, **22**, 18830; (d) K. Pei, Y. Wu, W. Wu, Q. Zhang, B. Chen, H. Tian and W. Zhu, *Chem. Eur. J*., 2012, **18**, 8190; (e) K. Pei, Y. Wu, A. Islam, Q. Zhang, L. Han, H. Tian and W. Zhu, *ACS Appl. Mater. Interfaces*, 2013, **5**, 4986; (f) H. Li, T. M. Koh, A. Hagfeldt, M. Grätzel, S. G. Mhaisalkar and A. C. Grimsdale, *Chem. Commun*., 2013, **49**, 2409; (h) J. Yang, P. Ganesan, J. Teuscher, T. Moehl, Y. J. Kim, C. Yi, P. Comte, K. Pei, T. W. Holcombe, M. K. Nazeeruddin, J. Hua, S. M. Zakeeruddin, H. Tian and M. Grätzel, *J. Am. Chem. Soc*., 2014, **136**, 5722; (i) C. A. Richard, Z. Pan, A. Parthasarathy, F. A. Arroyave, L. A. Estrada, K. S. Schanze and J. R. Reynolds, *J. Mater. Chem. A*, 2014, **2**, 9866; (j) L.-P. Zhang, K.-J. Jiang, G. Li, Q.-Q. Zhang and L.-M. Yang, *J. Mater. Chem. A*, 2014, **2**, 14852; (k) K. Pei, Y. Wu, A. Islam, S. Zhu, L. Han, Z. Geng and W. Zhu, *J. Phys. Chem. C*, 2014, **118**, 16552; (l) X. Lu, X. Jia, Z.-S. Wang and G. Zhou, *J. Mater. Chem. A*, 2013, **1**, 9697; (m) X. Lu, Q. Feng, T. Lan, G. Zhou and Z.-S. Wang, *Chem. Mater*., 2012, **24**, 3179.
16 N. Wang, Z. Chen, W. Wei and Z. Jiang, *J. Am. Chem. Soc*., 2013, **135**, 17060.
17 N. Blouin, A. Michaud, D. Gendron, S. Wakim, E. Blair, R. Neagu-Plesu, M. Belletête, G. Durocher, Y. Tao, and M. Leclerc, *J. Am. Chem. Soc.*, 2008, **130**, 732.
18 D. Milstein and J. K. Stille, *J. Am. Chem. Soc.*, 1978, **100**, 3636.
19 A. Vilsmeier and A. Haack, *Ber*., 1937, **60**, 119.
20 N. Miyaura and A. Suzuki, *Chem. Rev.*, 1995, **95**, 2457.
21 E. Knoevenagel, *Justus Liebigs Ann. Chem.*, 1894, **281**, 25.
22 A. Hagfeldt, G. Boschloo, L. Sun, L. Kloo and H. Pettersson, *Chem. Rev*., 2010, **110**, 6595.
23 M. J. Frisch, G. W. Trucks, H. B. Schlegel, G. E. Scuseria, M. A. Robb, J. R. Cheeseman, J. A. Montgomery, T. Vreven, K. N. Kudin, J. C. Burant, J. M. Millam, S. S. Iyengar, J. Tomasi, V. Barone, B. Mennucci, M. Cossi, G. Scalmani, N. Rega, G. A. Petersson, H. Nakatsuji, M. Hada, M. Ehara, K. Toyota, R. Fukuda, J. Hasegawa, M. Ishida, T. Nakajima, Y. Honda, O. Kitao, H. Nakai, M. Klene, X. Li, J. E. Knox, H. P. Hratchian, J. B. Cross, V. Bakken, C. Adamo, J. Jaramillo, R. Gomperts, R. E. Stratmann, O. Yazyev, A. J. Austin, R. Cammi, C. Pomelli, J. W. Ochterski, P. Y. Ayala, K. Morokuma, G. A. Voth, P. Salvador, J. J. Dannenberg, V. G. Zakrzewski, S. Dapprich, A. D. Daniels, M. C. Strain, O. Farkas, D. K. Malick, A. D. Rabuck, K. Raghavachari, J. B. Foresman, J. V. Ortiz, Q. Cui, A. G. Baboul, S. Clifford, J. Cioslowski, B. B. Stefanov, G. Liu, A. Liashenko, P. Piskorz, I. Komaromi, R. L. Martin, D. J. Fox, T. Keith, M.A. Al-Laham, C.Y. Peng, A. Nanayakkara, M. Challacombe, P. M. W. Gill,

B. Johnson, W. Chen, M. W. Wong, C. Gonzalez, J. A. Pople, Gaussian 03, Revision C.02, Gaussian, Inc., Wallingford, CT, 2004.
24 K. Hara, M. Kurashige, Y. Dan-oh, C. Kasada, A. Shinpo, S. Suga, K. Sayama, H. Arakawa, *New J. Chem.*, 2003, **27**, 783.
25 (a) T. Marinado, K. Nonomura, J. Nissfolk, M. K. Karlsson, D. P. Hagberg, L. Sun, S. Mori and A. Hagfeldt, *Langmuir*, 2009, **26**, 2592; (b) J. Bisquert, D. Cahen, G. Hodes, S. Rühle and A. Zaban, *J. Phys. Chem. B*, 2004, **108**, 8106; (c) Z. Ning, Y. Fu and H. Tian, *Energy Environ. Sci.*, 2010, **3**, 1170.
26 N. W. Duffy, L. M. Peter, R. M. G. Rajapakse and K. G. U. Wijayantha, *J. Phys. Chem. B*, 2000, **104**, 8916.



 

Table of Contents Entry

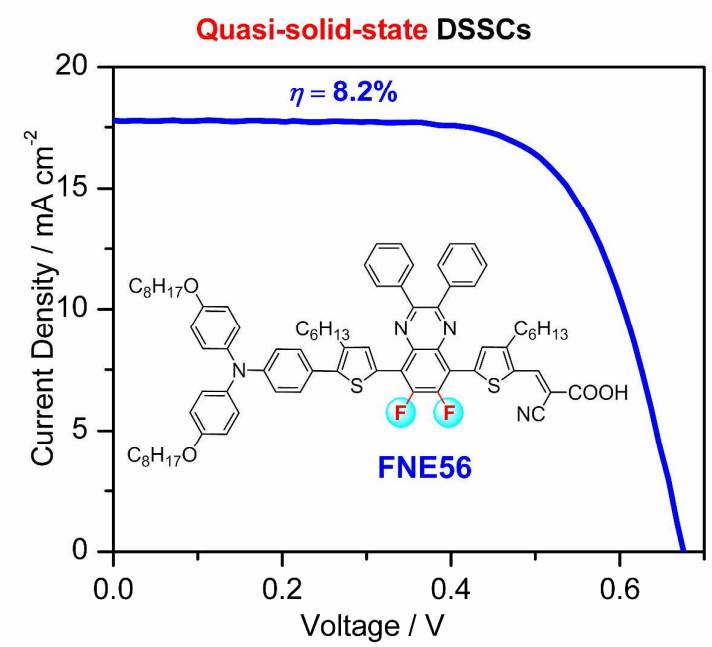


Two organic sensitizers containing fluorinated quinoxaline moiety have been designed and synthesized for efficient quasi-solid-state dye-sensitized solar cells.